Wiley
International Transactions on Electrical Energy Systems
Volume 2024, Article ID 5851912, 12 pages
https://doi.org/10.1155/2024/5851912

WILEY

Research Article

Intelligent Renewable Energy Agent-Based Distributed Control Design for Frequency Regulation and Economic Dispatch

Amjad Khan,[1] **Amjad Ullah Khattak**,[1] **Bilal Khan**,[2] **Sahibzada Muhammad Ali**,[2] **Zahid Ullah**,[3] **and Faisal Mehmood**[2]

[1]*Department of Electrical Engineering, University of Engineering and Technology, Peshawar, Pakistan*
[2]*Department of Electrical and Computer Engineering, COMSATS University Islamabad, Abbottabad Campus, Abbottabad, Pakistan*
[3]*Dipartimento di Elettronica, Informazione e Bioingegneria, Politecnico di Milano, Milano 20133, Italy*

Correspondence should be addressed to Bilal Khan; bilalkhan@cuiatd.edu.pk and Zahid Ullah; zahid.ullah@polimi.it

Received 15 December 2023; Revised 29 March 2024; Accepted 29 June 2024

Academic Editor: Marcos Tostado-Véliz

The Distributed Renewable Energy Sources (DRESs) integrate hybrid microgrid and prosumer activities that constitute a dynamic system characterized by unknown network parameters. The dynamic system faces challenges, such as intermittent power supply due to low inertia, renewable intermittence, plug-and-play prosumer activities, network topology variations, and a lack of constraint handling. These complexities pose significant issues in designing effective control for frequency regulation and consensus-based economic load dispatch (ELD) within DRES to meet varying load demands. To address the above challenges, this research employs a machine learning-based distributed multiagent consensus design that offers a rapid and robust approach, mitigating the limitations associated with the Distributed Average Integral (DAI) control design. The proposed multiagent scheme empowers the successful implementation of ELD and frequency regulation, accommodating the intermittent DRES, diverse network topologies, and the dynamic plug-and-play activities of prosumers. Moreover, an optimization-based DAI tuning model is introduced to overcome tuning limitations. Intelligent renewable energy agents are trained through machine learning-based regression models that use root mean square error metrics for performance evaluations. The intelligent agents employ DAI control to overcome inherent limitations. The effectiveness of the machine learning-based DAI is thoroughly evaluated using the DRES-based IEEE 14-bus hybrid microgrid system. The quantitative results prove its efficacy in addressing the complex challenges of integrated microgrid dynamics.

1. Introduction

Global warming significantly impacts human lives, including power demand, food security, biodiversity, water resources, human lifestyles, and the world economy. Due to global warming and fossil fuel depletion in the energy sector, the future power grid will rely heavily on renewable energy sources and prosumer activities [1, 2]. Over the last few decades, research in the power sector shifted towards nonconventional and green economical energy generation solutions to improve the penetration of renewable energy sources and provide an industrial revolution to overcome economic crises and reduce environmental degradation [3]. The penetration of renewable energy provides a distributed decentralized power production, shifting from centralized controlled energy productions [4]. The control design for distributed decentralized power production further divides power system operations into microgrid (MG) for local load satisfaction [5]. To facilitate the new power system operations, efficient control is required for optimum power management and stability of MG due to low rotational inertia and intermittence of renewable energy sources [6, 7].

The penetration of Distributed Renewable Energy Sources (DRESs) has introduced new avenues for control design, including addressing renewable intermittence, plug-and-play capabilities, and power quality. Moreover, MG demands fast responses with low inertia. Therefore, a significant transition from a centralized to a distributed control scheme is pivotal for the reliable and sustainable operation of the power system [8]. The power generated by DRES within the MG is either DC or variable AC, necessitating a power electronic interface to ensure the desired power quality [9]. To simulate the electric performance of a conventional power grid, a hierarchical control scheme is employed in the MG [10]. The hierarchical control architecture comprises three levels: primary, secondary, and tertiary control, which differ in their infrastructure, communication methods, time frame, and speed of response [11]. The primary control layer facilitates active and reactive power sharing among inverters, swiftly responding to deviations. It leads to frequency and voltage deviations, necessitating the secondary layer to minimize these deviations. This layer regulates the frequency and voltage by injecting power from the DRES. At the highest level, the tertiary control manages economic dispatch operations and coordinates multiple interfacing MGs [12, 13]. Traditionally, this highest level of control (tertiary) follows a master-slave approach. A central controller, acting as a cognitive agent in the master-slave relationship, communicates directly with distributed units to establish a control plan [14, 15]. The centralized scheme for economic dispatching, crucial for the optimal operation of MG, necessitates a complex communication framework between various DRES and central control units [14]. However, the centralized control methodology introduces several operational and reliability issues due to a single communication link, which may compromise the power system's stability. Therefore, distributed control emerges as the most effective way to overcome the aforementioned challenges while ensuring MGs' economical and reliable operation [16]. Model Predictive Control- (MPC-) based strategies for optimal energy management systems are investigated for a centralized design approach to maximize the utilization of renewable penetration in MG [16, 17].

The distributed control methodology implies paralleling control functions in the absence of global network information. Thus, distributed control techniques, with reduced computational burden and local communication, may assist in integrating DRES into the MG [18]. A variety of distributed economic dispatch control solutions are proposed in the literature, spanning both the secondary and tertiary control levels. The control designs may be classified into Distributed Average Integral (DAI) [19, 20] and model-based control designs [21, 22]. The DAI control design assumes sufficiently large power generation to deal with production constraints using DRES and presumes infinite bandwidth for the communication network. However, these design schemes provide control without considering the parametric dynamics and topologies of the power dynamic systems. Consequently, the DAI control design exhibits a sluggish response and is incapable of handling the uncertainties of power system dynamics and inherent intermittence of renewable energy sources [21, 22]. Furthermore, the heuristic control tuning techniques associated with DAI control degrade performance due to sluggish behavior [23]. Distributed control relies on communication networks and time-dependent dynamics, leading to significant literature focusing on finite control design [24].

To optimize resource management in islanded MGs, a multiagent consensus-based energy management system is developed [25]. However, conventional distributed economic dispatch schemes struggle to handle the faster dynamics introduced by the nonlinearity of renewable penetration and the topological aspects of the power system. Furthermore, model-based designs prove sensitive to model and system parameters. Consequently, renewables' variable power injection ability leads to new emerging concepts of volatile constraints in control problems [26, 27]. Notably, in the literature, novel methodologies such as Secondary Distributed MPC, employing the construction of virtual power models, demonstrate promise despite being associated with the shortcomings of an ideal communication network in these solutions [21, 28].

Due to the heterogeneous physical nature of DRES within MG, the massive penetration of renewable distributed generation in the power grid poses challenges in deploying control strategies even within the architecture of distributed control designs. Detailed physical modeling is limited due to the nonlinear and stochastic nature of the growing heterogeneous power network, compromising the accurate estimation of power demands. These inherent topological variations further create new challenges in the domain of economic dispatch within MGs. Recently, machine learning techniques have been adopted to solve distributed economic dispatch problems, employing cooperative reinforcement learning [29]. The authors in [30] developed a consensus transfer Q-learning algorithm for two-layer decentralized generation dispatch commitment in automatic generation control. Moreover, a distributive approach presents reinforcement learning-based economic dispatching [31]. Thus, this article addresses the compromised estimation of power demands using enhanced machine learning-based DAI controllers in a distributed manner.

Therefore, this paper proposes an intelligent multiagent MG control method based on machine learning algorithms with the underlying objectives of frequency regulation and an optimized economic dispatch scheme. The research focuses specifically on a supervised machine learning decision-making framework, in which a well-trained intelligent multiagent model is adopted at the local distributed agent to drive the DAI control law. The proposed data-driven, machine learning-based, intelligent multiagent approach in MG is aimed at minimizing costs while satisfying power demands and maintaining frequency regulation. The major contributions of this article are outlined as follows:

(i) An optimization scheme is proposed for tuning DAI gains, providing frequency regulation and power consensus to achieve economic load dispatch. The formulation also considers power production constraints.

(ii) To facilitate the unconstrained economic load dispatch consensus, a machine learning-assisted DAI is developed to satisfy power generation constraints.

(iii) Considering the effects of renewable intermittence and plug-and-play prosumer activities (which introduce a dynamic communication network among DRES), economic load dispatch might encounter challenges. An intelligent renewable energy agent drives the DAI towards dynamic power consensus to overcome the aforementioned issue, thereby achieving economic dispatch.

This paper is organized as follows. Section 2 provides background information on the mathematical modeling of MG, the MG communication model, control design objectives, and the DAI control law. Section 3 presents the proposed optimization formulation for DAI control tuning. Section 4 introduces an intelligent-based multiagent design that supports the control law. Section 5 outlines the machine learning-assisted DAI control design. Section 6 includes the performance evaluation of the proposed control design. Finally, Section 7 concludes the paper.

2. Mathematical Modeling of Microgrid

In traditional power systems, the majority of power production is generated by fossil-based large synchronous generators. The drive towards a low carbon footprint and green energy motivates the penetration of renewable energy sources (DRES) and prosumers (individuals motivated to inject surplus power into the grid) [5]. DRES and numerous power injection units, including energy storage elements and electric vehicles, aimed to fulfill peak-hour power demands [6]. Consequently, an efficient control design becomes imperative for power system stability and optimal operation. A hierarchical control architecture is designed for MG, incorporating DRES with advanced communication, monitoring, and computational technologies. This architecture aims to ensure frequency regulation, voltage regulation, cost-effectiveness, and optimal power sharing among DRES to meet the power load demands.

2.1. Microgrid Power Network Model. The power network of the MG comprises power generation units, DRES, or energy storage elements injecting power into the system to meet the load demand (p_{LL}). Second-order dynamics are integrated into the primary control to simulate the second-order swing equation of synchronous generators [6, 19]. The second-order dynamics of the i_{th} power generation unit are presented below [19–21]:

$$\begin{aligned}\dot{\theta}_i &= \omega_i,\\ m_i\dot{\omega}_i &= -d_i\left(\omega_i-\omega_d\right)-p_i+u_i.\end{aligned} \tag{1}$$

In (1), $\theta_i \in \mathbb{R}$ represents the phase, and $\omega_i \in \mathbb{R}$ represents the angular frequency of the DRES in the MG. Meanwhile, $m_i \in \mathbb{R} > 0$ represents the virtual inertia, and $d_i \in \mathbb{R} > 0$ denotes the damping of the DRES. The desired angular frequency is $w_d \in \mathbb{R} > 0$, and the secondary control is denoted by $u_i \in \mathbb{R}$. The power injection by the DRES is represented by $u_i \in \mathbb{R}$, which is the sum of power consumed by the local load $(p_{\text{LL},i})$ and the power delivered to the power network $(p_{n,i})$ expressed as follows [19–21]:

$$\begin{aligned}p_i &= p_{\text{LL},i}+p_{n,i},\\ p_{n,i} &= \sum_{j\in N_p} y_{ij}\left(v_i^2\cos\left(\theta_{z,ij}\right)-v_iv_j\cos\left(\theta_{z,ij}+\theta_i-\theta_j\right)\right).\end{aligned} \tag{2}$$

In (2), j represents neighboring power nodes within the set of N_p power nodes. The power flow among these nodes is a nonlinear sinusoidal function dependent on y_{ij} impedance, voltages v_i and v_j, the phase angle of impedance $\theta_{z,ij}$, and the phase of the i^{th} and j^{th} power nodes denoted as θ_i and θ_j, respectively. The deviation variables are represented as $\Delta\omega_i = \omega_i - \omega_d$ and $\Delta\theta_i = \theta_i - \omega_d t$.

2.2. Microgrid Communication Network Model. The communication network for an MG is modeled using graph theory. A connected static graph is represented by $\mathbb{G}$, consisting of a set $N = n_1, \ldots, n_n$ containing n nodes. We consider a connected graph for the power system's communication modeling. In $\mathbb{G}$, the power nodes are denoted by N_p, and the load nodes are denoted by N_L, where $N = N_p \cup N_L$ and $N_p \cap N_L = \varnothing$. The topology of the connected network is represented by a symmetric adjacency matrix $A \in \mathbb{R}^{n\times n} \geq 0$. The graph is connected through branches, and each communication connection between nodes n_i and n_j is represented by an element of A: $a_{ij} = 1$, while $a_{ij} = 0$ indicated otherwise.

The communication model is designed using the Laplacian matrix of A, defined using the degree matrix as follows: $Q \coloneqq D(A1_n)$ and $\mathscr{L} \coloneqq \mathscr{Q} - A$, where $\mathscr{L} \in \mathbb{R}^{n\times n}$.

2.3. Control Design Objectives. The two control design objectives for distributed secondary control are frequency regulation and economic load dispatch based on identical cost criteria [32].

$$\begin{aligned}\Delta\omega_i(t) &= 0 \quad \left(\forall i \in N_p\right),\\ \sum_{j\in N_{c,i}}\left(c_ip_i-c_jp_j\right) &= 0 \quad \left(\forall i,j \in N_p\right).\end{aligned} \tag{3}$$

In (3), c_i and c_j represent the production cost of the i^{th} and j^{th} nodes, respectively, while $N_{c,i}$ represents the set of i^{th} neighboring communication nodes.

2.4. Distributed Average Integral. The DAI control design aims to achieve both objectives: frequency regulation and economic load dispatch [19, 20, 23]. This control design is developed based on the deviation in frequency regulation (similar to the standard power oscillation damping regulation problem) and deviation in economically dispatched power, utilizing communication links and production cost. Several researchers proposed the DAI control design by integrating the gains of frequency and economic load dispatch errors of local and neighboring loads using communication links.

The mathematical formulation of DAI control law is provided as follows [19, 20]:

$$\dot{u}_i = -k_w(\omega_i - \omega_d) - k_p \sum_{j\in N_{c,i}} \left(N_{c,i}c_i p_i - c_j p_j\right), \tag{4}$$

where $k_w \in \mathbb{R}$ and $k_p \in \mathbb{R}$ are tuning parameters. k_w gain for oscillation damping and k_p gain create consensus using communication between nodes to achieve an economic power dispatch.

3. Optimization Scheme for DAI Control Tuning

The DAI controller successfully achieves both control goals: frequency regulation and economic load dispatch. However, DAI controller is implemented without identifying the system dynamics. The DAI controller design is based on a few approximations:

(i) The controller is designed based on an unlimited supply of power at each node to fulfill the load demand.

(ii) An unconstrained economic load dispatch problem is implemented for controller design.

These limitations become apparent in scenarios involving renewable energy penetration and plug-and-play prosumer activities. Machine learning-based agent design is employed to address these limitations. In this section, we propose an optimization formulation to tune the gains of DAI, considering system dynamics and power generation constraints.

An optimization formulation is proposed to identify the DAI gains values for each node.

$$\begin{aligned} &\min . \int_0^T \|\Delta\omega\|_Q^2 + \lambda \left\| N c_i p_i - \sum_{j=1}^{N} c_j p_j \right\|_S^2, \\ &\text{Subject to} \quad m_i\dot{\omega}_i = -d_i(\omega_i - \omega_d) - p_i + u_i, \dot{u}_i = -k_w(\omega_i - \omega_d) - k_p \sum_{j\in N_{c,i}} \left(N_{c,i}c_i p_i - c_j p_j\right), p_{i,\min} \le p_i \le p_{i,\max}. \end{aligned} \tag{5}$$

The objective function aims to achieve both oscillation damping and economic load dispatch. The optimization formulation relies on system dynamics, which are dependent on both the power and communication network. Inequality constraints are integrated to address the limitations of the DAI controller, particularly its reliance on unlimited power availability. In renewable generation, issues such as renewable intermittence and variations in power generation commonly arise. To overcome the limitations of DAI, we propose implementing intelligent agents at each node using a machine learning model.

4. Intelligent-Based Multiagent Design

A multiagent system (MAS) comprises multiple autonomous renewable generation agents that interact to achieve economically dispatched power load demands. The MAS collaborates to enhance power system scalability and plug-and-play flexibility. MAS includes economic dispatch goals, power generation information from self and neighboring renewable agents, and a DAI controller to inject the desired power into the power network.

4.1. Machine Learning-Based Multiagent Design. In the MAS architecture, the DAI controller provides oscillation damping and economic power dispatch through cooperation among MAS entities and consistent power network dynamics. However, this architecture faces issues like renewable intermittence, power generation saturation, and the dynamic plug-and-play activities of renewable generations. These challenges compromise the economic dispatch and power consensus of renewable generations. To address these issues, we propose an intelligent MAS architecture (illustrated in Figure 1) using a machine learning model to supervise the DAI controller and provide the necessary control actions.

The machine learning model of an intelligent agent provides updated power error consensus information to the DAI controller. This facilitates injecting the desired power into the network to enable power dispatch and oscillation damping, considering dynamic variations within the power network.

4.2. Machine Learning Model for Intelligent Agent. A Gaussian process regression (GPR) model is introduced to support the DAI control law for frequency regulation and economic dispatch. This model is probabilistic and nonparametric, based on kernels, and involves a finite number of random variables following a multivariate normal distribution. The GPR regression model establishes relationships between a node's power p_i, neighboring node's power p_j where $j \in N_c$, power node constraints $p_{i,\max}$ and $p_{i,\min}$, and economic dispatch error $\sum_{j\in N_{c,i}} (N_{c,i}c_i p_i - c_j p_j)$.

The linear regression model is formulated as [33]

$$y = \mathbf{x}^T \beta + \epsilon, \tag{6}$$

where β is a regression estimation parameter of linear model, x is the input vector, and y is the output of the model. The observation y is different from output due to additive error ϵ. The additive error is assumed to be an independent identically distributed Gaussian distribution with zero mean and variance σ^2, i.e., $\epsilon \sim \mathcal{N}(0, \sigma^2)$.

The probability density of σ^2 in terms of observation y given input x and parameter β is given by [33]

$$\begin{aligned} f(\epsilon) &= \frac{1}{\sqrt{2\pi\sigma}} \exp\left(-\frac{\epsilon^2}{2\sigma^2}\right), \\ \Rightarrow f(y \mid \mathbf{x}; \beta) &= \frac{1}{\sqrt{2\pi\sigma}} \exp\left(-\frac{\left(y - \mathbf{x}^T \beta\right)^2}{2\sigma^2}\right). \end{aligned} \tag{7}$$

As ϵ represents an error term assumed to be random, its probability density is depicted in equation (7). This term is introduced into the model to capture unmodeled effects within the dynamic power system.

4.3. Estimation of Regression Model. A supervised learning approach involves training and estimating the regression model using a set of known inputs and observations obtained from the system. The training of the GPR model dataset is presented as follows [33]:

$$\left\{(\mathbf{X}, \mathbf{Y}) = \left(\mathbf{x}_i, y_i\right) \forall i = 1, \ldots, n, \text{such that } \mathbf{x}_i \in \mathbb{R}^m, \quad y_i \in \mathbb{R}\right\}, \tag{8}$$

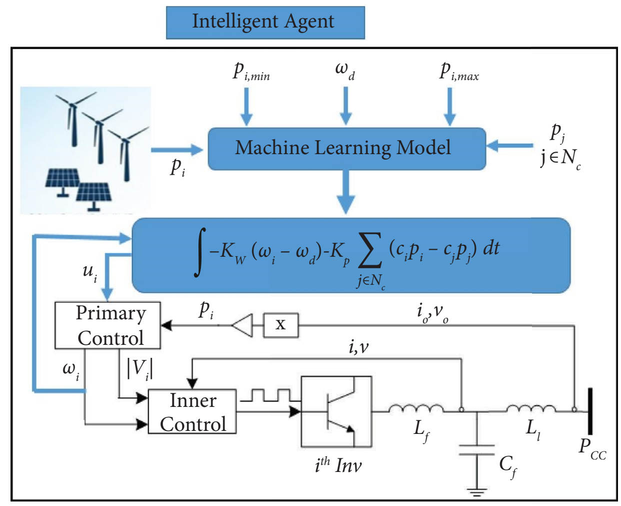

Figure 1: Intelligent renewable agent.

where m is the number of inputs and n is the number of observations. To estimate the parameter β, consider the likelihood function for dataset in (8) as [33]

$$L(\beta) = \prod_{i=1}^{n} \frac{1}{\sqrt{2\pi\sigma}} \exp\left(-\frac{\left(y_i - \mathbf{x}_i^T \beta\right)^2}{2\sigma^2}\right). \tag{9}$$

According to the principle of maximum likelihood, the best estimate of β is calculated by maximizing $L(\beta)$. To maximize $L(\beta)$, we considered the convex maximization of the log-likelihood $l(\beta)$, that is,

$$l(\beta) = \log \prod_{i=1}^{n} \frac{1}{\sqrt{2\pi\sigma}} \exp\left(-\frac{\left(y_i - \mathbf{x}_i^T \beta\right)^2}{2\sigma^2}\right) = n \quad \log \frac{1}{\sqrt{2\pi\sigma}} - \frac{1}{\sigma^2} \cdot \frac{1}{2} \sum_{i=1}^{n} \left(y_i - \mathbf{x}_i^T \beta\right)^2. \tag{10}$$

The maximization $l(\beta)$ is formulated to a convex unconstrained quadratic optimization problem formulation in parameter β. The optimization problem may be solved using least squares formulation as [33]

$$\beta = \left(\mathbf{X}^T \mathbf{X}\right)^{-1} \mathbf{X}^T \mathbf{Y}. \tag{11}$$

This will estimate the β parameter to model the GPR model using dataset in (8).

5. Machine Learning-Assisted DAI Control Design

The local control at each node is implemented using an intelligent-based multiagent design, leveraging local measurements and information obtained from neighboring nodes. All measurements are input into the GPR machine learning model, which generates the desired error input based on variations in the inputs driven by power system dynamic changes. These dynamic variations encompass renewable intermittence, plug-and-play prosumer activity, dynamic communication network alterations, and power generation constraints. The trained GPR model predicts the error input for the DAI controller, aiming to achieve frequency regulation and economic dispatch. The modified DAI control block diagram is illustrated in Figure 2.

In Figure 2, the communication between nodes occurs through a communication network, facilitating the exchange of information between neighboring power nodes and sharing local node measurements. The neighboring information and local measurements are transmitted to the GPR model, generating the desired error for frequency regulation and predicting the DAI controller's economic dispatch error. Once the error is calculated by the GPR model, the DAI controller utilizes this information to generate control signals, injecting the desired power into the power system.

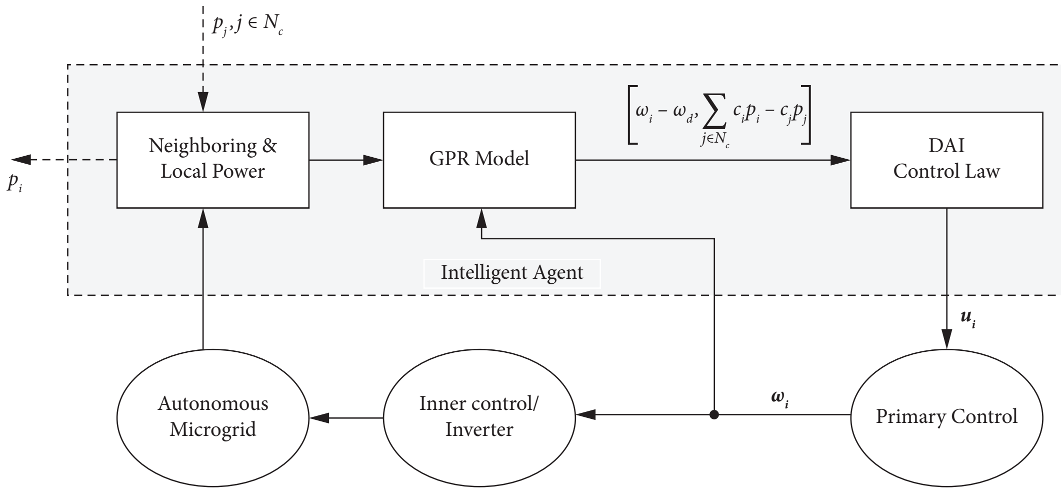

Figure 2: Block diagram of proposed DAI controller.

6. Performance Evaluation

The effectiveness of the proposed machine learning-based control design is assessed using the IEEE 14-bus power system depicted in Figure 3, and a comparison is made with the DAI controller.

An autonomous microgrid is represented by the IEEE 14-bus system, consisting of six power generation nodes: $N_p = n_1, n_2, n_3, n_6, n_8, n_{13}$. The simulation setup utilizes parameter data provided in the Appendix.

The multiobjective optimization was conducted using genetic algorithms in MATLAB, employing a population size of 50. The aim was to determine the optimal gain values for K_p and K_w to solve equation (5). Subsequently, the optimized tuning gain values for the DAI algorithm were identified as $K_p = 560$ and $K_w = 57140$.

6.1. Dataset for Machine Learning Model. The dataset is prepared for machine learning model training using the IEEE 14-bus system simulation data shown in Figure 3. Different scenarios are generated using 10 thousand samples. The DAI controller is designed for each scenario, injecting the desired power to meet control goals. The data needed to generate the required power injection are obtained by implementing the desired control design with optimal performance for each scenario, as depicted in Figure 4. In different scenarios, the communication topology also changes during the plug-out and plug-in of power nodes. This variation in communication generates fluctuations in economic dispatch error, illustrated in Figure 5. This dataset is used to train a Gaussian regression model that assists DAI control in achieving the desired control goals.

6.2. Training Intelligent Renewable Energy Agents. The training process involves the use of Gaussian process regression (GPR), whose kernel function represents the covariance between data points x_i and x_j, parameterized by θ. These hyperparameters are determined based on the signal deviation and the maximum allowed length of the response value, regulating the behavior of the kernel. Typically, the radial basis function kernel (also known as the squared exponential kernel) from the scikit-learn Gaussian process library is used.

To assess the effectiveness of GPR, it is compared with various regression models, including linear regression, random forest regression, support vector regression, and K-nearest neighbor regression. Figure 6 displays the fitting results of the Gaussian process and the residual plots of the different regression models. Comparisons are made based on key performance metrics such as root mean square error (RMSE), mean absolute error (MAE), and R^2 scoring metrics, as shown in Table 1. These metrics provide insights into a model's predictive accuracy and its ability to capture underlying patterns in the data.

Table 1 contains performance metrics for the various machine learning models used in the analysis. Each row corresponds to a specific model, and each column represents a performance metric: root mean square error (RMSE), mean absolute error (MAE), and coefficient of determination (R^2). The values in the table represent the performance of each model according to their respective metrics. For example, the Gaussian process model has an RMSE value of 0.0113, a MAE value of 0.0004, and an R^2 value of 0.0319. These metrics help evaluate each model's accuracy and goodness of fit to the data. Lower values of RMSE and MAE indicate better accuracy, while higher values of R^2 indicate a better fit of the model to the data.

Based on the analysis of the provided performance metrics in Table 1, GPR emerges as the preferred choice for this regression task. Its reliability and precision in modeling the relationship between input features and the target variable make it well-suited for training intelligent renewable energy agents. By minimizing prediction errors and accurately capturing underlying patterns, GPR facilitates robust and efficient decision making in renewable energy applications.

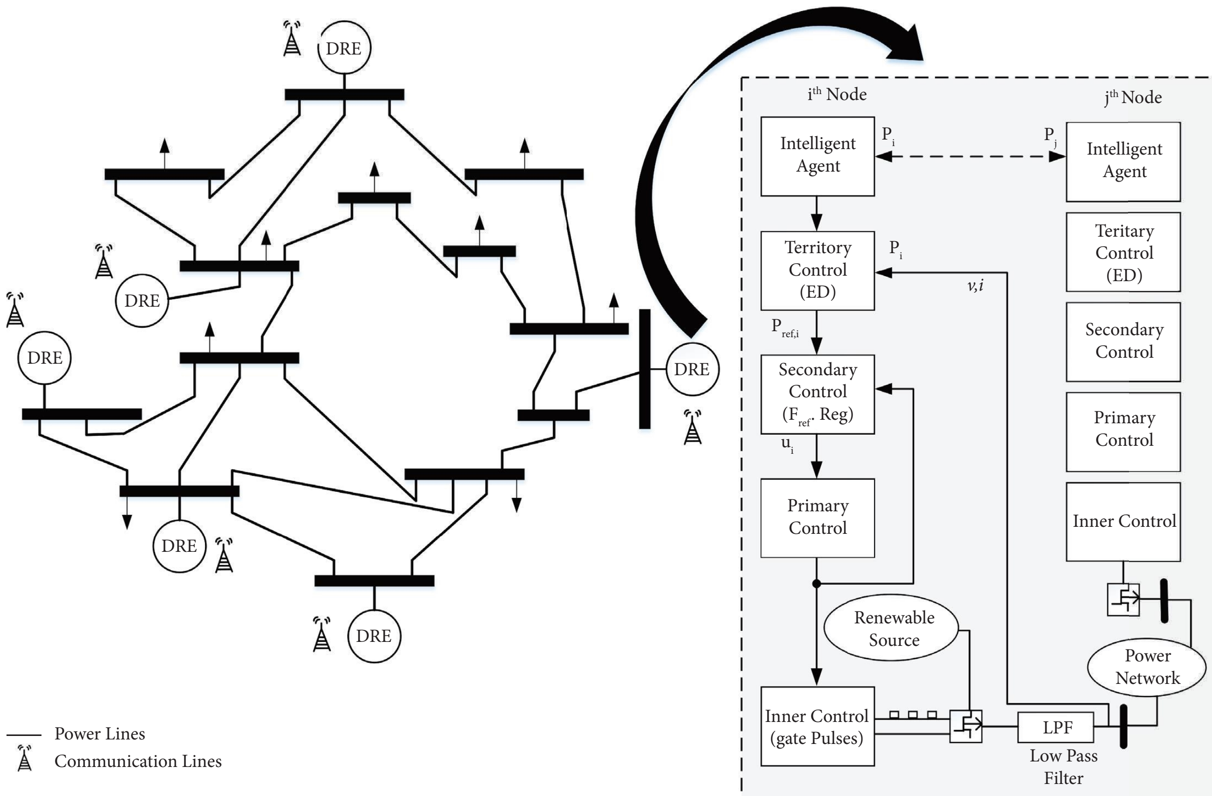

Figure 3: IEEE 14-bus power system for performance evaluation.

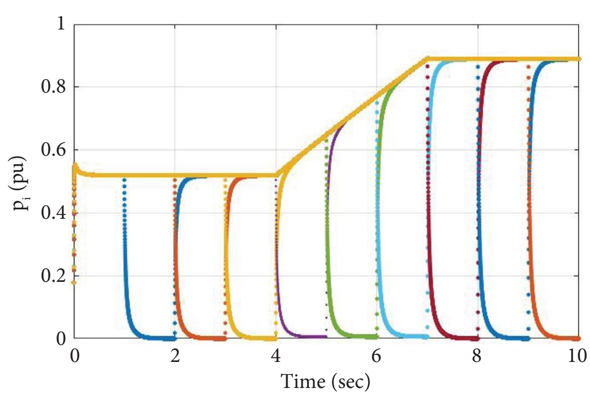

Figure 4: Power injection of power node 1 at multiple plug-in and plug-out scenarios of IEEE 14-bus power system.

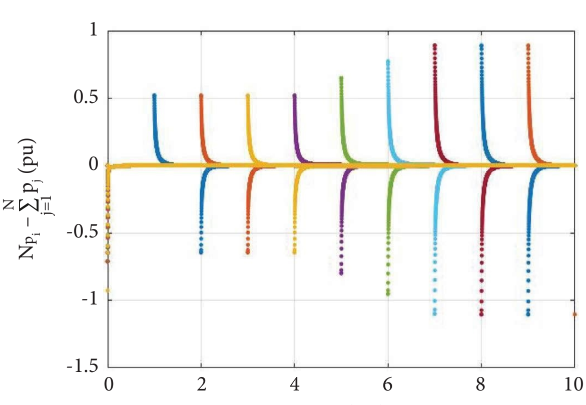

Figure 5: Economic load dispatch error variation of power of scenarios in Figure 4 of IEEE 14-bus power system.

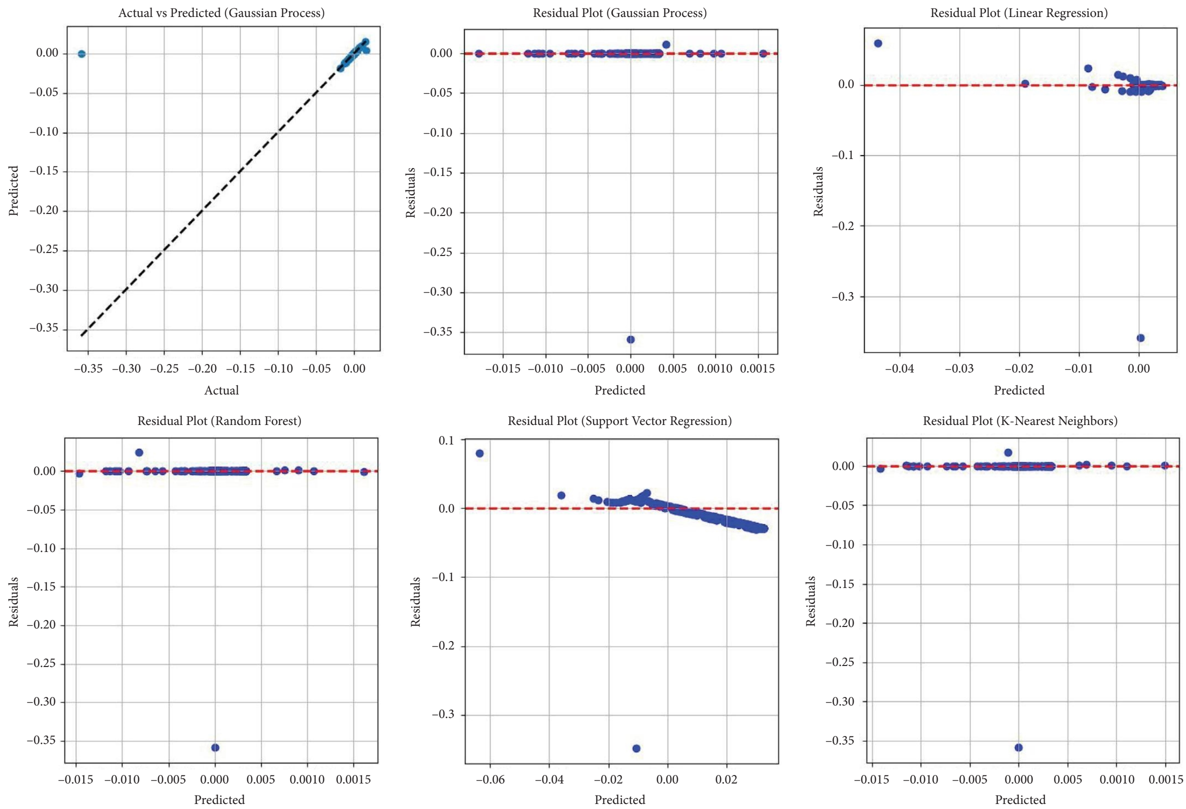

Figure 6: Gaussian process regression training and residual plot of Gaussian process, linear regression, random forest, support vector, and K-nearest neighbor regression models.

Table 1: Training performance metrics of Gaussian process, linear regression, random forest, support vector, and K-nearest neighbor regression models.

Model	RMSE	MAE	R^2
Gaussian process	0.0113	0.0004	0.0319
Linear regression	0.0116	0.0009	−0.0111
Random forest	0.0114	0.0004	0.0285
Support vector	0.0188	0.0141	−1.6492
K-nearest neighbors	0.0114	0.0004	0.0306

6.3. Performance Analysis of Intelligent Agent-Assisted DAI Control. The efficacy of the proposed design is evaluated through three different test scenarios. These scenarios include handling constraints related to DRES, plug-out and plug-in events, renewable intermittence, and communication link failures. The DAI control design is utilized to provide a benchmark for comparison. The simulations are carried out within a 10 ms time frame considering varying load demands.

6.4. DRES Generation Constraint Handling. The load demand remains constant for the constraint handling scenario until 1 ms. After 1 ms, the load starts increasing linearly until 3 ms, and then it remains constant until 10 ms. In this situation, generation node 1 has a limited production capacity of 0.6 pu, while the other nodes are assumed to have sufficiently large generation limits.

Figure 7 illustrates the power consensus using the intelligent agent-based DAI control design. During simulation, around 1.63 ms, generation node 1 becomes saturated, hitting its maximum generation limit and unable to increase its power output further. As a result, this node exits the consensus while the remaining nodes continue to work towards incremental power consensus to attain the economic load dispatch objective. In the DAI case, the constraint information related to power production remains unknown, leading to a decline in performance. Figure 8 depicts the incremental power consensus process. As power generation node 1 gets saturated, the other nodes are unable to converge towards a consistent incremental power consensus. This highlights the constraint of the DAI control design, a limitation that the intelligent agent-based DAI control design successfully overcomes.

6.5. Power Intermittence Using Plug-In and Plug-Out of DRES. Renewable power generation exhibits inherent phenomena of intermittent power generation and plug-in/plug-out activity. To simulate these phenomena, power generation node 1 is disconnected at 2 ms and then reconnected at 4 ms. This scenario effectively models power generation intermittence as well as the activity of connecting and disconnecting renewable generation.

In Figure 9, the economic dispatch consensus is represented using intelligent agents. When node 1 is disconnected due to intermittence, the intelligent agent detects the

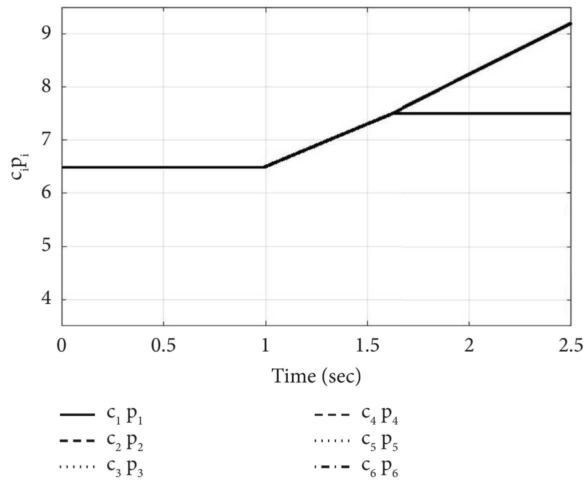

FIGURE 7: Identical incremental power cost using intelligent agent-based DAI design under node 1 power saturation.

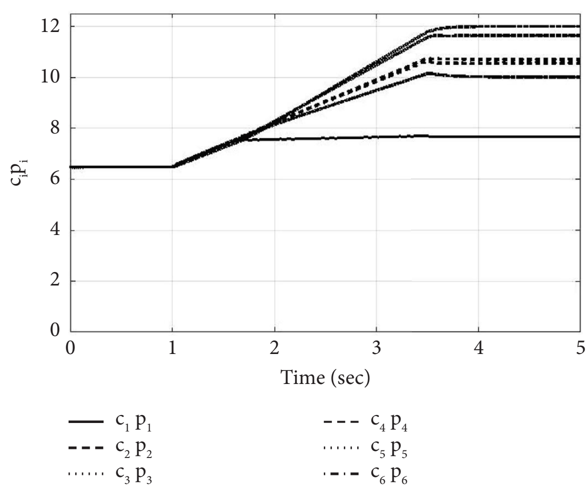

FIGURE 8: Identical incremental power cost using classical DAI design under node 1 power saturation.

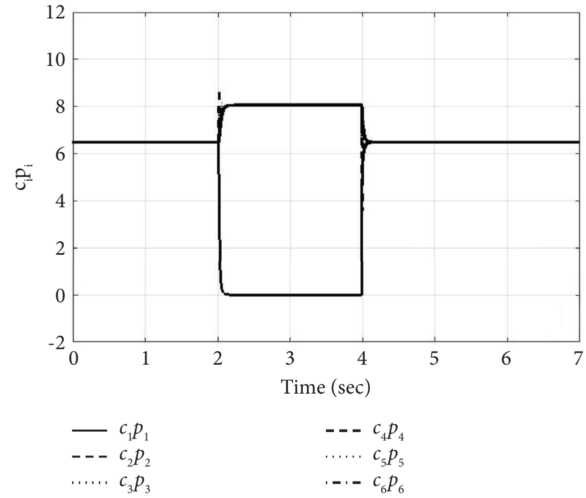

FIGURE 9: Identical economic dispatch consensus using intelligent agent-based DAI design under node 1 plug-in/plug-out power generation.

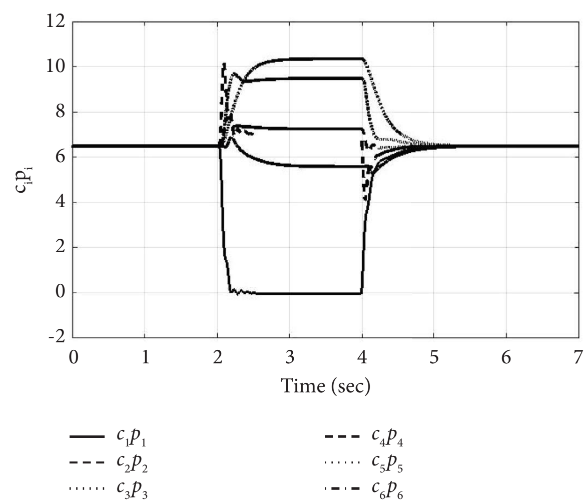

FIGURE 10: Economic dispatch consensus using classical DAI design under node 1 power intermittence.

dynamic change and updates the error information for the DAI control to establish a new economic dispatch consensus. Similarly, at 4 ms, when power node 1 is reconnected, this introduces another dynamic variation that is also managed by the intelligent agent designed using the DAI controller. In contrast, as shown in Figure 10, the DAI controller fails to identify the dynamic variation, resulting in a failure to achieve economic dispatch consensus. However, the DAI controller successfully reestablishes consensus when node 1 is reconnected at 4 ms. The classical DAI design is incapable of achieving economic dispatch during instances of plug-in/plug-out or intermittent power generation.

6.6. Power Communication Link Failure. The DAI control design relies on the communication network to establish communication with neighboring nodes and utilizes information from neighboring nodes to achieve economic dispatch. In the context of this simulation scenario, we investigate the impact of communication link failure on economic dispatch consensus. At 5 ms, the communication link between node 3 and node 4 becomes disrupted. Despite this link failure, both nodes continue to inject power owing to the interconnected dynamics of the power system. Regrettably, the breakdown in the link between node 3 and node 4 leads to an inaccurate error calculation for the economic dispatch process.

In Figure 11, the intelligent agent promptly detects the link failure, leading to a variation in error calculation. Based on machine learning principles, the DAI design adapts to this variation after 5 ms and successfully maintains the ongoing economic dispatch consensus. In contrast, as shown in Figure 12, the conventional DAI system fails to compensate for the link failure and the subsequent change in communication topology. As a result, the economic dispatch objective remains unachieved using the DAI approach after the 5 ms mark.

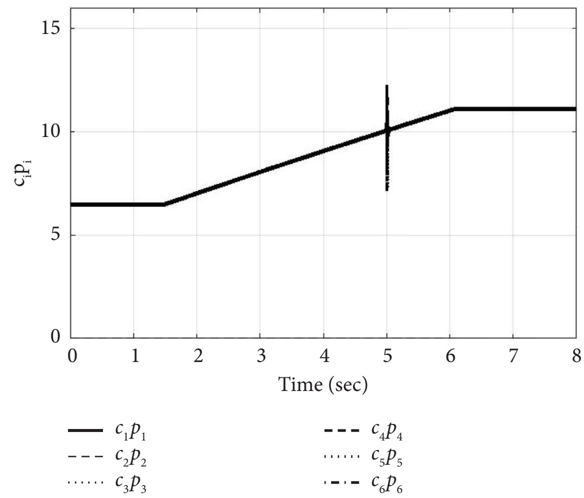

FIGURE 11: Economic dispatch using intelligent agent-based DAI design under node 1 communication link failure.

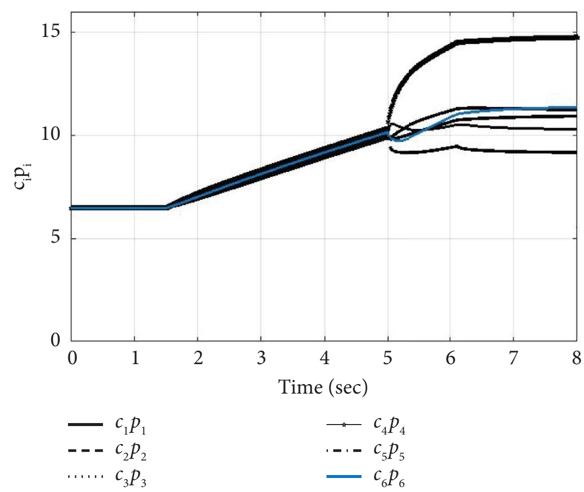

FIGURE 12: Economic dispatch using classical DAI design under node 1 communication link failure.

6.7. Comparative Performance Analysis of Control Design. In Table 2, a comparative analysis is provided for incremental power cost consensus across constraint handling, power intermittence, and communication link failure scenarios to analyze the performance of intelligent agent-based DAI and classical DAI. The performance is evaluated across nodes labeled as P_1 through P_6, utilizing achieved consensus values, absolute error, and relative error as metrics.

In all scenarios, intelligent agent-based DAI outperforms classical DAI in terms of both absolute and relative error metrics. For example, under the constraint handling scenario, intelligent agent-based DAI achieves lower absolute and relative errors compared to classical DAI across all nodes (P_1 to P_6). This trend remains consistent in the power intermittence and communication link failure scenarios as well. These findings indicate that the intelligent agent-based DAI controller exhibits superior performance in maintaining power consensus and mitigating errors, making it a more effective choice for managing dynamic and complex situations in power systems.

TABLE 2: Comparative performance analysis of incremental power cost consensus across different scenarios.

Constraint handling	P1	P2	P3	P4	P5	P6
Intelligent agent-based DAI	7.502	11.08	11.08	11.08	11.08	11.08
Classical DAI	7.667	10.55	11.63	10.71	11.99	10.02
Absolute error	0.165	0.53	0.55	0.37	0.91	1.06
Relative error (%)	2.19	4.78	4.96	3.34	8.21	9.57
Power intermittence	**P1**	**P2**	**P3**	**P4**	**P5**	**P6**
Intelligent agent-based DAI	70	8.052	8.052	8.052	8.052	8.052
Classical DAI	0	6.884	9.477	7.251	10.33	5.596
Absolute error	0	1.168	1.425	0.801	2.278	2.456
Relative error (%)	0	14.50	17.70	9.95	28.29	30.50
Communication link failure	**P1**	**P2**	**P3**	**P4**	**P5**	**P6**
Intelligent agent-based DAI	11.12	11.12	11.12	11.12	11.12	11.12
Classical DAI	10.56	9.2	11.32	14.73	10.93	11.36
Absolute error	0.56	1.92	0.2	3.61	0.19	0.24
Relative error (%)	5.04	17.27	1.80	32.46	1.71	2.16

7. Conclusion and Future Directions

The classical DAI design faces challenges in adapting dynamic variations, such as plug-in/plug-out scenarios during renewable intermittence and the saturation of power generation due to power generation constraints. Moreover, the conventional DAI approach struggles to detect communication link failures or variations in communication topology. The DAI control scheme is designed to operate effectively under specific conditions including consistent power system dynamics, fixed power network topology, stable communication topology, reliable communication platforms, and unconstrained power generation. However, these constraints limit its applicability in diverse scenarios. The DAI design leverages machine learning models within an intelligent agent framework to overcome these limitations. This intelligent agent requires a comprehensive dataset for training and enabling to overcome the inherent constraints of conventional DAI control design. In the proposed approach, the DAI control design integrated the principles of multiagent learning. This integration empowered the control system to adapt and perform optimally with rapid dynamic environments. Combining the strengths of machine learning and intelligent agents, the proposed approach potentially overcame the challenges associated with classical DAI design and achieved enhanced performance.

This approach will merge model-based design and data-driven control design to accommodate the complex dynamics of power systems, while simultaneously designing the control law using a limited dataset.

Appendix

A. IEEE 14-Bus Test System

Damping factor: $D = [1.61.22.32.11.54.8]$.
Virtual inertia: $M = [5.223.984.494.225.44.5]$.
Cost rates: $C = [12.515102017.516.5]$ $(cost/pu^2)$.
Production constraints: $P_{\min} = \mathbf{0}_6$.
$P_{\max} = [0.600.851.300.700.800.62]$, (pu).

B. DAI Parameters

Tuning Parameters for DAI: $K_p = 560$ and $K_w = 57140$.

Nomenclature

$\lambda \in \mathbb{R}$:	Weighting parameter
$\sigma^2 \in \mathbb{R}$:	Variance
$L(\beta) \in \mathbb{R}$:	Likelihood function
$l(\beta) \in \mathbb{R}$:	Log-likelihood function
$\beta \in \mathbb{R}$:	Parameter of linear model
$\mathbf{x} \in \mathbb{R}^n$:	Model input
$\omega_i \in \mathbb{R}$:	Angular frequency
$\theta_i \in \mathbb{R}$:	Instantaneous phase
$c_i p_i \in \mathbb{R}$:	Incremental cost
$d_i \in \mathbb{R}$:	Damping factor
k_w & $k_p \in \mathbb{R}$:	Tuning parameters of DAI
$m_i \in \mathbb{R}$:	Rotational inertia
$N_{c,i} \in \mathbb{R}$:	Set of neighboring nodes in terms of communication links
$N_p \in \mathbb{R}$:	Set of power nodes
$p_i \in \mathbb{R}$:	Instantaneous power injection
$p_{i,\min}$ & $p_{i,\max} \in \mathbb{R}$:	Power injection limits
$p_{LL,i} \in \mathbb{R}$:	Local load of power node
$p_{n,i} \in \mathbb{R}$:	Power flow onto neighboring nodes
Q & $S \in \mathbb{R} > 0$:	Penalty matrices
$u_i \in \mathbb{R}$:	Secondary control input
$v_i \in \mathbb{R}$:	Voltage of power node
$w_d \in \mathbb{R}$:	Desired synchronous angular frequency
$y \in \mathbb{R}$:	Output of the model
y_{ij} & $z_{ij} \in \mathbb{R}$:	Admittance and impedance of power line.

Data Availability

The data used to support the findings of the study are available from the corresponding authors upon request.

Conflicts of Interest

The authors declare that they have no conflicts of interest.

Authors' Contributions

A. Khattak and B. Khan were responsible for conceptualization. A. Khan was responsible for methodology. S. M. Ali, A. Khattak, and B. Khan were responsible for validation. A. Khan and Z. Ullah were responsible for formal analysis. F. Mehmood was responsible for investigation, data curation, and software. B. Khan and Z. Ullah were responsible for resources. A. Khattak was responsible for supervision. Z. Ullah was responsible for funding acquisition. All authors have read and agreed to the published version of the manuscript.

Acknowledgments

The authors would like to thank the Politecnico di Milano for support APC under CARE-CRUI Agreement.

References

[1] A. G. Olabi and M. A. Abdelkareem, "Renewable energy and climate change," *Renewable and Sustainable Energy Reviews*, vol. 158, Article ID 112111, 2022.

[2] W. Ahmed, B. Khan, Z. Ullah et al., "Stochastic adaptive-service level agreement-based Energy Management Model for smart grid and Prosumers," *PLoS One*, vol. 17, no. 12, p. e0278324, 2022.

[3] C. Xue, M. Shahbaz, Z. Ahmed, M. Ahmad, and A. Sinha, "Clean Energy Consumption, economic growth, and environmental sustainability: what is the role of economic policy uncertainty?" *Renewable Energy*, vol. 184, pp. 899–907, 2022.

[4] Y. Huo and G. Gruosso, "Hardware-in-the-loop framework for validation of ancillary service in microgrids: feasibility, problems and improvement," *IEEE Access*, vol. 7, pp. 58104–58112, 2019.

[5] N. Shaukat, S. M. Ali, C. A. Mehmood et al., "A survey on consumers empowerment, communication technologies, and renewable generation penetration within Smart Grid," *Renewable and Sustainable Energy Reviews*, vol. 81, pp. 1453–1475, 2018.

[6] B. Shaker, K. Ullah, Z. Ullah, M. Ahsan, M. Ibrar, and M. A. Javed, "Enhancing grid resilience: leveraging power from flexible load in modern Power Systems," in *Proceedings of the 2023 18th International Conference on Emerging Technologies (ICET)*, Peshawar, Pakistan, November 2023.

[7] S. M. Ali, M. Jawad, B. Khan et al., "Wide area smart grid architectural model and control: a survey," *Renewable and Sustainable Energy Reviews*, vol. 64, pp. 311–328, 2016.

[8] T. Khalili and A. Bidram, "Distributed control approaches for Microgrids," *Micro*, vol. 23, pp. 275–288, 2021.

[9] M. E. Souza Junior and L. C. Freitas, "Power electronics for modern sustainable power systems: distributed generation, microgrids and smart grids—a review," *Sustainability*, vol. 14, no. 6, p. 3597, 2022.

[10] R. Zamora and A. K. Srivastava, "Multi-layer architecture for voltage and frequency control in networked microgrids," *IEEE Transactions on Smart Grid*, vol. 52, p. 1, 2016.

[11] A. Mohammed, S. S. Refaat, S. Bayhan, and H. Abu-Rub, "AC microgrid control and management strategies: evaluation and review," *IEEE Power Electronics Magazine*, vol. 6, no. 2, pp. 18–31, 2019.

[12] Y. Khayat, Q. Shafiee, R. Heydari et al., "On the secondary control architectures of AC Microgrids: an overview," *IEEE Transactions on Power Electronics*, vol. 35, no. 6, pp. 6482–6500, 2020.

[13] C. Zhao, E. Mallada, and F. Dorfler, "Distributed frequency control for stability and economic dispatch in Power Networks," in *Proceedings of the 2015 American Control Conference (ACC)*, Chicago, IL, USA, June 2015.

[14] L. Ding, Q. L. Han, and X. M. Zhang, "Distributed secondary control for active power sharing and frequency regulation in islanded microgrids using an event-triggered communication mechanism," *IEEE Transactions on Industrial Informatics*, vol. 15, no. 7, pp. 3910–3922, 2019.

[15] S. Das and A. K. Barik, "Opposition-based competitive swarm optimizer for optimal sizing and siting of DG units in Radial System," *Lecture Notes in Electrical Engineering*, vol. 63, pp. 269–282, 2022.

[16] A. Alqurashi, A. H. Etemadi, and A. Khodaei, "Model predictive control to two-stage stochastic dynamic economic dispatch problem," *Control Engineering Practice*, vol. 69, pp. 112–121, 2017.

[17] I. Prodan and E. Zio, "A model predictive control framework for reliable microgrid Energy Management," *International Journal of Electrical Power and Energy Systems*, vol. 61, pp. 399–409, 2014.

[18] T. R. Nudell, M. Brignone, M. Robba et al., "Distributed control for polygeneration microgrids: a dynamic market mechanism approach," *Control Engineering Practice*, vol. 121, Article ID 105052, 2022.

[19] J. Schiffer, F. Dörfler, and E. Fridman, "Robustness of distributed averaging control in power systems: time delays and Dynamic Communication Topology," *Automatica*, vol. 80, pp. 261–271, 2017.

[20] M. A. Rustam, B. Khan, S. M. Ali et al., "An adaptive distributed averaging integral control scheme for micro-grids with renewable intermittency and varying operating cost," *IEEE Access*, vol. 8, pp. 455–464, 2020.

[21] F. Mehmood, B. Khan, S. M. Ali, and J. A. Rossiter, "Distributed mpc for economic dispatch and intermittence control of renewable based autonomous microgrid," *Electric Power Systems Research*, vol. 195, Article ID 107131, 2021.

[22] F. Mehmood, B. Khan, S. M. Ali, and J. A. Rossiter, "Distributed model predictive based secondary control for economic production and frequency regulation of mg," *IET Control Theory and Applications*, vol. 13, no. 17, pp. 2948–2958, 2019.

[23] F. Dorfler, J. W. Simpson-Porco, and F. Bullo, "Breaking the hierarchy: distributed Control and economic optimality in microgrids," *IEEE Transactions on Control of Network Systems*, vol. 3, no. 3, pp. 241–253, 2016.

[24] G. Lou, W. Gu, X. Lu, Y. Xu, and H. Hong, "Distributed secondary voltage control in islanded microgrids with consideration of Communication Network and time delays," *IEEE Transactions on Smart Grid*, vol. 11, no. 5, pp. 3702–3715, 2020.

[25] T. Zhao and Z. Ding, "Distributed agent consensus-based optimal resource management for Microgrids," *IEEE Transactions on Sustainable Energy*, vol. 9, no. 1, pp. 443–452, 2018.

[26] Y. Qiu, J. Lin, F. Liu, and Y. Song, "An explicit MPC based on Galerkin method for AGC considering Volatile Generations," in *Proceedings of the 2019 IEEE Power and Energy Society General Meeting (PESGM)*, Atlanta, GE, USA, September 2019.

[27] Y. Xu, Z. Dong, Z. Li, Y. Liu, and Z. Ding, "Distributed optimization for integrated frequency regulation and economic dispatch in Microgrids," *IEEE Transactions on Smart Grid*, vol. 12, no. 6, pp. 4595–4606, 2021.

[28] F. Mehmood, B. Khan, S. M. Ali, M. B. Qureshi, C. Diver, and R. Nawaz, "Multi-renewable energy agent based control for economic dispatch and frequency regulation of autonomous renewable grid," *IEEE Access*, vol. 8, pp. 89534–89545, 2020.

[29] W. Liu, P. Zhuang, H. Liang, J. Peng, and Z. Huang, "Distributed economic dispatch in microgrids based on cooperative reinforcement learning," *IEEE Transactions on Neural Networks and Learning Systems*, vol. 29, no. 6, pp. 2192–2203, 2018.

[30] X. S. Zhang, Q. Li, T. Yu, and B. Yang, "Consensus transfer Q-learning for decentralized generation command dispatch based on Virtual Generation Tribe," *IEEE Transactions on Smart Grid*, vol. 23, p. 1, 2016.

[31] P. Dai, W. Yu, G. Wen, and S. Baldi, "Distributed reinforcement learning algorithm for dynamic economic dispatch with unknown generation cost functions," *IEEE Transactions on Industrial Informatics*, vol. 16, no. 4, pp. 2258–2267, 2020.

[32] J. Schiffer and F. Dorfler, "On stability of a distributed averaging pi frequency and active power controlled differential-algebraic power system model," in *Proceedings of the 2016 European Control Conference (ECC)*, Aalborg, Denmark, June 2016.

[33] S. Kanwal, B. Khan, S. M. Ali, and C. A. Mehmood, "Gaussian process regression based inertia emulation and reserve estimation for grid interfaced photovoltaic system," *Renewable Energy*, vol. 126, pp. 865–875, 2018.